

## Foot-and-Mouth Disease Virus Mutant with Decreased Sensitivity to Ribavirin: Implications for Error Catastrophe<sup>∇</sup>

Macarena Sierra, Antero Airaksinen,† Claudia González-López,¶ Rubén Agudo, Armando Arias, and Esteban Domingo\*

*Centro de Biología Molecular Severo Ochoa (CSIC-UAM), Cantoblanco, E-28049 Madrid, Spain*

Received 27 July 2006/Accepted 23 November 2006

**The nucleoside analogue ribavirin (R) is mutagenic for foot-and-mouth disease virus (FMDV). Passage of FMDV in the presence of increasing concentrations of R resulted in the selection of FMDV with the amino acid substitution M296I in the viral polymerase (3D). Measurements of progeny production and viral fitness with chimeric viruses in the presence and absence of R documented that the 3D substitution M296I conferred on FMDV a selective replicative advantage in the presence of R but not in the absence of R. In polymerization assays, a purified mutant polymerase with I296 showed a decreased capacity to use ribavirin triphosphate as a substrate in the place of GTP and ATP, compared with the wild-type enzyme. The results suggest that M296I has been selected because it attenuates the mutagenic activity of R with FMDV. Replacement M296I is located within a highly conserved stretch in picornaviral polymerases which includes residues that interact with the template-primer complex and probably also with the incoming nucleotide, according to the three-dimensional structure of FMDV 3D. Given that a 3D substitution, distant from M296I, was associated with resistance to R in poliovirus, the results indicate that picornaviral polymerases include different domains that can alter the interaction of the enzyme with mutagenic nucleoside analogues. Implications for lethal mutagenesis are discussed.**

RNA viruses do not replicate as informationally defined genomes but as complex and dynamic mutant spectra termed viral quasispecies (11, 24, 25, 29, 30). Several relevant biological properties of RNA viruses as infectious agents depend on aspects of their mutant spectra: (i) the association of disease outcome with the complexity (quantitated by average mutation frequencies and genetic distances) of the mutant spectra (33, 34, 59–61, 63, 64, 75), (ii) complementation among components of a mutant spectrum that can mediate virus spread and pathogenesis (53, 76), and (iii) suppression of specific variants by the surrounding mutant spectrum (23, 41, 42, 47), which can attenuate the disease potential of a virus (14, 73; for general reviews on implications of quasispecies, see references 24, 25, 27, and 38).

An application of quasispecies dynamics has been the development of a new antiviral strategy termed virus entry into error catastrophe or lethal mutagenesis (2, 10, 28, 29, 51, 71). Firmly rooted in the theoretical studies (reviewed in references 10 and 28), the concept of virus extinction through error catastrophe has been amply supported by experimental studies with RNA viruses (reviewed in references 2 and 27). Stated in general terms, for any replication system there is a maximum error rate

above which the genetic information carried by the system can no longer be maintained (2, 27, 28). Several recent observations have strengthened error catastrophe as a feasible new antiviral strategy. (i) The mutagenic nucleoside analogue ribavirin (1-β-D-ribofuranosyl-1,2,4-triazole-3-carboxamide) (R), an antiviral agent licensed for clinical practice (58, 69), is mutagenic for a number of RNA viruses (16, 18, 19, 21, 50, 67), including foot-and-mouth disease virus (FMDV) (1, 56). Recent evidence suggests that R can act as a mutagen for hepatitis C virus in the course of treatment of chronically infected patients (9). Therefore, in some viral infections, R may exert its antiviral effect, in part, via its mutagenic activity (44, 45, 58). (ii) The mutagenic base analogue 5-fluorouracil prevented the establishment of a persistent infection of mice with lymphocytic choriomeningitis virus (65). This experiment constitutes a proof of the principle of the feasibility of an error catastrophe-based antiviral approach *in vivo*. (iii) Mutagenesis—not merely inhibition of viral replication—drives viruses to extinction (55).

The mutagenic activity of R with poliovirus is exerted after its intracellular conversion to the triphosphate form (RTP), which is incorporated by the poliovirus RNA-dependent RNA polymerase (RdRp), termed 3D, and acts as a mutagenic purine analogue (17–19). By growing poliovirus in the presence of R, a poliovirus mutant with the replacement G64S in 3D was selected (62, 76). This mutant (3D G64S) shows a decreased capacity to use RTP as a substrate and an increased template copying fidelity, as measured by genetic and biochemical methods (8, 12, 62, 75). Poliovirus mutant 3D G64S has been instrumental on several grounds. (i) RdRps are the major viral gene products responsible of the error-prone replication and quasispecies dynamics of RNA viruses. Therefore, fidelity mutants are essential for studying the molecular basis of template-copying fidelity, designing fidelity-lowering drugs, and explor-

\* Corresponding author. Mailing address: Centro de Biología Molecular Severo Ochoa (CSIC-UAM), Cantoblanco, E-28049 Madrid, Spain. Phone: 34 91 4978485. Fax: 34 91 4974799. E-mail: edomingo@cbm.uam.es.

† Present address: National Product Control Agency for Welfare and Health, Chemicals Unit, PL 210, FI-00531 Helsinki, Finland.

¶ Present address: Cell Biology Unit, MRC-Laboratory for Molecular Cell Biology, and Department of Biochemistry and Molecular Biology, University College London, Gower Street, London WC1E 6BT, United Kingdom.

<sup>∇</sup> Published ahead of print on 6 December 2006.

ing the influence of mutation rates on virus behavior. (ii) Poliovirus mutant 3D G64S has documented that enhanced fidelity need not entail a decreased replication rate, that a broad mutant spectrum is essential for virus adaptation to a complex environment (in this case represented by susceptible mice [61, 75]), and that an individual mutant unable to reach a target organ can do so when complemented by a population displaying a broad mutant spectrum (61, 76). These are essential features of quasispecies behavior which have now become amenable to direct experimental analysis *in vivo*. (iii) The poliovirus mutant 3D G64S has revealed that viruses with increased resistance to nucleoside analogues can be isolated and, therefore, that such mutants could contribute to failures of lethal mutagenesis as an antiviral strategy.

The fact that two groups working independently selected the same R-resistant poliovirus mutant, 3D G64S (62, 76), suggests that picornaviral polymerases may have very limited possibilities for circumventing the selective disadvantage associated with the mutagenic activity of R. Because of the new avenues for understanding RNA genetics that have been opened by the R-resistant poliovirus mutant, and since R acts also as a mutagenic agent for FMDV (1, 56), we designed experiments to select FMDV mutants with decreased sensitivity to R. Here we describe the isolation of a new class of picornavirus mutants displaying decreased sensitivity to R. The FMDV mutant harbors the M296I substitution in 3D and was selected in the course of passage of FMDV in BHK-21 cells in the presence of increasing concentrations of R. We document that the M296I replacement confers on FMDV a selective advantage during replication in the presence of R and that the purified mutant 3D has an impaired capacity, relative to that of the wild-type enzyme, to incorporate RTP in the place of GTP opposite to a C and in the place of ATP opposite to a U in the template. In the three-dimensional structure of FMDV 3D, M296 is located far from position G62 (the amino acid equivalent of G64 in poliovirus 3D) but lies within a conserved amino acid stretch that establishes contacts with the template-primer RNA and probably also with the incoming nucleotide substrate (35–37). The implications of the isolation of the FMDV mutant 3D M296I for selection of extinction escape mutants and a possible failure of an error catastrophe-based antiviral approach are discussed.

#### MATERIALS AND METHODS

**Cells, viruses, and infections.** The origin of BHK-21 cells and procedures for cell growth and infection of cell monolayers with FMDV in liquid medium and in semisolid agar medium for plaque assays have previously been described (26, 70). FMDV C-S8c1 is a plaque-purified derivative of natural isolate C<sub>1</sub> Santa-Pau Spain 70 (70), a representative of European serotype C FMDV. FMDV MARLS is a monoclonal antibody escape mutant selected from the C-S8c1 population passaged 213 times in BHK-21 cells (13). The fitness of MARLS relative to that of C-S8c1 has been estimated at 25 from previous data (39, 57).

**Treatment with ribavirin.** A solution of R in phosphate-buffered saline was prepared at a concentration of 200 mM, sterilized by filtration, and stored at  $-20^{\circ}\text{C}$ . Prior to use, the stock solution was diluted in Dulbecco's modification of Eagle's medium to reach the desired concentrations. Cell monolayers were incubated for 7 h with R prior to infection. Infected cells in the absence of R and mock-infected cells were maintained in parallel; no evidence of contamination of cells with virus was observed at any time. FMDV MARLS was passaged serially in the presence and absence of increasing concentrations (200  $\mu\text{M}$  to 800  $\mu\text{M}$ ) of R (Fig. 1); virus rescued from infectious transcripts of pMT28 and pMT28-3D(M296I) (described below) were passaged serially five times in the absence or in the presence of ribavirin (800  $\mu\text{M}$ ). For each passage,  $4 \times 10^6$  BHK-21 cells

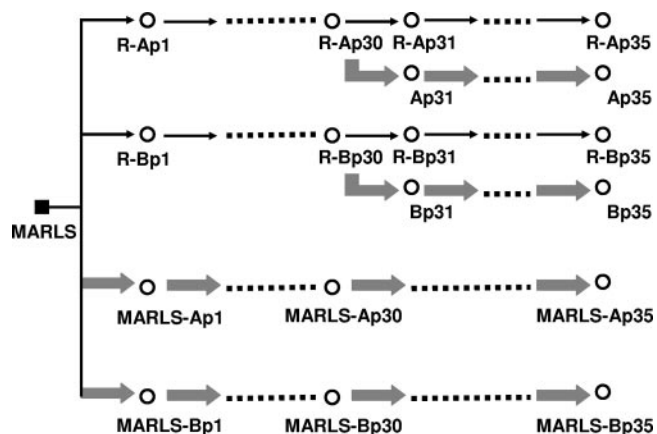


FIG. 1. Scheme of passages of FMDV MARLS in the presence or absence of R. The initial biological clone MARLS (filled square) was subjected to four parallel passage series; empty circles indicate the uncloned progeny FMDV populations. Thin arrows indicate passages in the presence of R (with duplicate lineages R-A and R-B; passages 1 to 5 were with 200  $\mu\text{M}$  R, passages 6 to 25 were with 400  $\mu\text{M}$  R, and passages 25 to 35 were with 800  $\mu\text{M}$  R). Large arrows indicate passages in the absence of R (duplicate lineages MARLS-A and MARLS-B); “p” followed by a number refers to passage number. The origin of FMDV MARLS and conditions for the infection of BHK-21 cell monolayers in the presence or absence of R are described in Materials and Methods.

were infected with  $1 \times 10^6$  to  $4 \times 10^6$  PFU of virus from the previous passage until cytopathology was complete (about 30 h in the presence of R and 16 h in the absence of R).

**Extraction of RNA, cDNA synthesis, PCR amplification, and nucleotide sequencing.** RNA was extracted from the supernatants of infected cells by treatment with Trizol (Invitrogen) as previously described (68). Reverse transcription (RT) was carried out using avian myeloblastosis virus reverse transcriptase (Promega), and PCR amplification was performed using AmpliTaq polymerase (Perkin-Elmer) as specified by the manufacturer. RT-PCR amplifications intended for the cloning of individual cDNA molecules were carried out using *Pfu* DNA polymerase (Promega) because of its high copying fidelity (15), using primers and procedures that have been described previously (1, 39, 55, 57, 68); experimental details will be provided upon request. Nucleotide sequencing was carried out using the Big Dye Terminator cycle sequencing kit (ABI Prism; Perkin-Elmer) and an automated ABI 373 sequencer; all sequences were determined at least in duplicate from independent sequencing reaction mixtures. The nucleotide sequences of the genomes of FMDV C-S8c1 and MARLS are available in GenBank, with accession numbers AJ133357 and AF274010, respectively.

**Quantification of viral RNA.** FMDV RNA was quantified by real-time RT-PCR amplification using the Light Cycler instrument (Roche) and the RNA Master SYBR green I kit (Roche) according to the instructions of the manufacturer. Quantification was relative to a standard curve obtained with known amounts of FMDV C-S8c1 RNA. This procedure has been described previously (40, 41).

**Molecular cloning, expression, and purification of FMDV 3D.** Molecular cloning of the FMDV genomic region encoding the viral polymerase (3D) in plasmid pET-28a, IPTG (isopropyl- $\beta$ -D-thiogalactopyranoside) induction of *Escherichia coli*, cell lysis, and enzyme purification by affinity chromatography through Nitrilotriacetic acid were carried out as previously described (37). The expression vector pET-28a including the wild-type FMDV 3D (with the 3D sequence of our standard FMDV C-S8c1) is termed pET-28a3D, and it has been described previously (3, 37). To clone and express 3D of MARLS and 3D of MARLS with the M296I replacement, cDNA from the corresponding FMDV genomes was amplified with EHF polymerase (Roche) and primers A2SaC1 ([CAGAGCTCG ACCCTGAACCGCACCACGA in the sense orientation; the 5' nucleotide is at position 6581; FMDV residue numbering is as described in reference 31) and C-not-pol (CCAATTGTGATGTTTGCGCGCCGCTGCGTCGCCGACACG GCGTTC in the antisense orientation; the 5' nucleotide is at FMDV C-S8c1 genomic position 8043). The product was digested with HindIII (genomic position 6667) and NotI (position 8020) (the restriction site generated with the

nucleotides is in boldface in primer C-not-pol) and ligated to plasmid pET-28a3D, which had been previously digested with the same enzymes and treated with shrimp alkaline phosphatase (66). The expression plasmid encoding 3D of FMDV MARLS is termed pET-28a3D(M). 3D of MARLS differs from 3D of C-S8c1 in having H instead of Q at position 232. The presence of H or Q at position 232 of 3D did not have any detectable effect either in the progeny production capacity of FMDV or in standard enzymological activities with purified 3D [polymerization with poly(A)-oligo(dT)<sub>15</sub>, VPg uridylylation, and RNA binding measured by gel mobility shift assay (3, 35, 37)]. The plasmid encoding 3D with the M296I substitution in the context of 3D of the MARLS (with Q232H) plasmid is termed pET-28a3D(M-M296I). The sequence of the 3D-coding region was confirmed for all constructs. The expressed 3D proteins are termed 3D(M) and 3D(M-M296I). The 3Ds were purified as previously described (37).

**Preparation of FMDVs with mutations in 3D.** Plasmid pMT28 encodes an infectious transcript of FMDV C-S8c1 (40). Chimeric plasmids encoding mutant 3Ds of the FMDV C-S8c1 genome were constructed by replacing part of the 3D-coding region of pMT28 with the corresponding 3D-coding region of the mutant of interest. Specifically, to construct pMT28-3D(M) (an infectious clone expressing 3D of MARLS in the context of the C-S8c1 genome), pMT28 was amplified with primer CR3DIL (GCGACAAAGGTTTGTCTTGG; the 5' nucleotide is at position 7718) and T7 (described in reference 3), and viral RNA encoding MARLS polymerase was subjected to RT-PCR amplification with avian myeloblastosis virus reverse transcriptase and *Pfu* DNA polymerase, using primers A2SacI and Av2New (TG TGAAGTGTCTTTGAGGAAAG; the 5' nucleotide is at position 7783). The two amplicons were shuffled and digested with ClaI (position 7004) and NdeI [the site of the restriction enzyme was engineered at the 3' side of the viral poly(A) (40)]. The digest was ligated to pMT28 DNA previously digested with the same enzymes. To construct pMT28-3D(M-M296I), RNA encoding M296I was subjected to the same procedure, except that the shuffled DNA product was digested with SalI (position 7150) and NdeI and the digestion product was ligated to pMT28 DNA that had been digested previously with SalI and NdeI. To construct pMT28-3D(M296I), the codon encoding Met 296 of the FMDV 3D polymerase was changed to Ile in wild-type pMT28. We replaced codon 296, ATG, with an alternative Ile codon, ATA, by site-directed mutagenesis during PCR amplification using the primer pair A2SacI and MKRES (GGAACAGCCAGATGGTAT; the 5' nucleotide is at position 7512; the underlined residue corresponds to the mutation site) and primer Forward ResA (GAAGGCGGGATACCATCTGGCTGTTCCG; the 5' nucleotide is at position 7486) with the T7 primer. The amplicons were shuffled, digested with NdeI and ClaI, and ligated to pMT28 DNA that had previously been digested with ClaI and NdeI.

Ligation, transformation of *E. coli* DH5 $\alpha$ , and colony screening with PCR amplification, nucleotide sequencing, and preparation of infectious RNA transcripts were carried out as previously described (3, 66). RNA concentrations of infectious transcripts were estimated by agarose gel electrophoresis and ethidium bromide staining, with known amounts of *E. coli* rRNA as the standard. About 1  $\mu$ g of FMDV RNA transcript were transfected into BHK-21 cells using lipofectin (Gibco), and cells were cultured until cytopathology was complete. Then the virus obtained was passaged twice in BHK-21 cells, and aliquots for further studies were prepared and stored at  $-70^{\circ}\text{C}$ . The entire 3D-coding regions of the resulting clonal populations were sequenced to confirm that their nucleotide sequences were identical to those of the corresponding parental plasmids.

**Characterization of mutant spectra.** The complexity of mutant spectra was determined by quantifying the mutation frequency, expressed as the number of different mutations divided by the total number of nucleotides sequenced, and by the normalized Shannon entropy, which is a measure of the proportion of identical sequences in a distribution (1, 55, 68). For populations Ap35 and Bp35 (Fig. 1), the residues of 3D that were analyzed spanned residues 7150 to 8020 and 7004 to 8020, respectively. For pMT28 and pMT28-3D(M296I) populations, the entire 3D- and VP1-coding regions were sequenced.

**Fitness assays.** Relative fitness was measured by growth competition experiments in the presence or absence of R, as previously described (4, 49). The proportion of the two competing genomes at different passages was determined by real-time RT-PCR, employing primers specifically designed to discriminate the two RNAs. The discriminatory forward primers were MKWT (GGAACAGCCAGATGGCAT) for pMT28-3D(M) and MKRES for pMT28-3D(M-M296I) (the 5' nucleotide is at position 7512 for both primers); the G7497A mutation (underlined nucleotide) is present only in the R-resistant genomes and corresponds to the M296I replacement in 3D. The reverse primer was 3DR4 (ACTCGCATGTGCGAGTTTT; the 5' nucleotide is at position 7141) in both cases. The hybridization temperature for real time RT-PCR assays was  $68^{\circ}\text{C}$  for wild-type and  $72^{\circ}\text{C}$  for mutant RNA. Under these conditions, amplification of the two

competing RNAs was accurately discriminated (4). To determine the relative fitness value, the logarithm of the ratio of the two competing RNAs was plotted against passage number to obtain the fitness vector; the antilogarithm of the vector slope is the fitness of the virus tested, relative to that of the reference virus (49).

**3D polymerization assays.** Polymerization assays were carried out using poly(rC) or poly(rU) (300 residues on average; Amersham Pharmacia) as templates and oligo(dG)<sub>15</sub> (Life Technologies) or oligo(rA)<sub>6</sub> (Dharmacon Research), respectively, as primers. The assay was performed with MOPS (morpholinepropanesulfonic acid; 30 mM, pH 7.0; Sigma), NaCl (33 mM), and Mg(CH<sub>3</sub>COO)<sub>2</sub> (15 mM) or MnCl<sub>2</sub> (10 mM) with poly(rC) or poly(rU) (40 ng/ $\mu$ l), oligo(dG)<sub>15</sub> or oligo(rA)<sub>6</sub> (2.4  $\mu$ M), [ $\alpha$ -<sup>32</sup>P]GTP or [ $\alpha$ -<sup>32</sup>P]ATP (20 mCi/mmol, 0.01 mCi/ml; Amersham), RTP (Moravek Biochemicals, Inc.), and 3D (3  $\mu$ M) (in Tris-HCl [250 mM, pH 7.5], NaCl [250 mM], EDTA [1 mM], glycerol [10%, vol/vol]). A 22.5- $\mu$ l mixture of all components except 3D was prewarmed for 2 min at  $37^{\circ}\text{C}$ , and the reaction was started by adding 2.5  $\mu$ l of 3D; the reaction was carried out for 10 or 30 min [for assays with poly(rC) or poly(rU), respectively] at  $37^{\circ}\text{C}$  and stopped by the addition of 5  $\mu$ l of 500 mM EDTA. Deviations from the basic protocol and specific concentrations of substrate and templates-primers are indicated in the corresponding figure legend. Reaction products were subjected to nucleotide analysis. To this aim, the reaction products were separated from unincorporated nucleotides using G25 Sephadex chromatography (Mini Quick Spin Oligo columns; Roche), equilibrated with Tris-HCl (10 mM, pH 8.0), EDTA (1 mM); the RNA was precipitated with ethanol, dissolved in water, and digested with a mixture of RNase A (500 ng/ $\mu$ l) (Boehringer Mannheim) and RNase T<sub>2</sub> (0.1 U/ $\mu$ l) (Sigma) for 15 min at  $37^{\circ}\text{C}$  in NH<sub>4</sub>(CH<sub>3</sub>COO)<sub>2</sub> (50 mM, pH 5.0). Mononucleotides were separated by polyethylenimine-cellulose thin-layer chromatography, using as the solvent 0.5% formic acid for the products with poly(rC) as the template or 0.75% formic acid for the products with poly(rU) as the template and Li-formate (0.15 M) adjusted to pH 3.0 with formic acid (77). The membranes were air dried and the reaction products analyzed and quantitated using a phosphorimager (model BAS-1500; Fuji).

3D polymerization assays with heteropolymeric templates were used to study the incorporation of nucleotides at a defined position. To this aim, symmetrical- and substrate-RNA (sym/sub-RNA) oligonucleotides (Dharmacon Research) (5) were purified, end labeled with [ $\gamma$ -<sup>32</sup>P]ATP and polynucleotide kinase (NEB), and annealed using standard protocols (5, 66). 3D (3  $\mu$ M) and sym/sub-C (5'-GUACGGCCCC-3') or sym/sub-U (5'-GCAUGGGCCCC-3') were incubated in MOPS (30 mM, pH 7.0), NaCl (33 mM), and Mg(CH<sub>3</sub>COO)<sub>2</sub> (15 mM) for 10 min at  $37^{\circ}\text{C}$  and then mixed with nucleoside triphosphate substrates (different ratios of RTP and GTP) to initiate the reaction (final volume, 25  $\mu$ l). Deviations from this basic protocol and specific concentrations of substrate and templates-primers are indicated in the figure legends. After 5 min, or at fixed times after the addition of the substrate, the reaction was stopped by the addition of EDTA to a final concentration of 83 mM. Reaction products were resolved by electrophoresis on a denaturing 23% polyacrylamide and 7 M urea gel in Tris base (90 mM), boric acid (90 mM), EDTA (2 mM) (pH 8.0). Proteins in gels were visualized and quantitated with a phosphorimager (model BAS-1500; Fuji).

**Other assays with 3D.** Poly(rU) synthesis using poly(A)-oligo(dT)<sub>15</sub> as the template-primer, VPg uridylylation, and RNA binding assays were carried out as previously described (3).

## RESULTS

**Selection of an FMDV mutant with decreased sensitivity to ribavirin.** R can eliminate FMDV from persistently infected BHK-21 cells (22), and its activity is, at least in part, exerted by lethal mutagenesis (1). To test whether FMDV with decreased sensitivity to R could be selected, FMDV MARLS (13) was passaged cytolytically in the presence of increasing concentrations of R. MARLS was chosen due to its high fitness (39) to favor a broad mutant spectrum on which selection could act. The passage protocol was designed to generate two parallel lineages of virus replicating in the presence of R and two ensuing bifurcations to continue replication in both the presence and absence of R; a control passage series was also used (Fig. 1). To test whether passage in the presence of increasing concentrations of R resulted in FMDV populations with de-

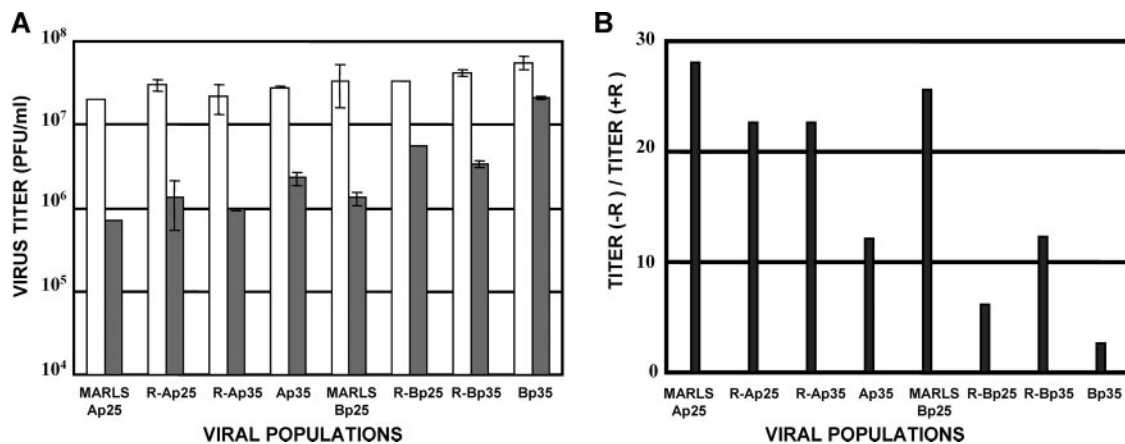


FIG. 2. FMDV titer produced in the presence or absence of R. (A) BHK-21 cell monolayers were infected at an MOI of 0.05 PFU/cell with the viral populations indicated in the abscissa (the passage history of the viruses is described in the legend to Fig. 1) either in the absence (empty bars) or presence (filled bars) of R (800  $\mu$ M). Virus was titrated when cytopathology was complete (16 to 30 h postinfection). Titrations were carried out in triplicate, and standard deviations are given. Procedures are described in Materials and Methods. (B) Ratios of titers of progeny virus produced in the absence to those produced in the presence of R, calculated from the results shown in panel A. Note the differences in the ratios between parallel passage series A and B (compare with Fig. 1). Procedures are described in Materials and Methods.

creased sensitivities to R, the capacity of several viral populations to produce progeny in the presence and absence of R was tested. The ratios of titers produced in the absence relative to the titers produced in the presence of R were 25 to 28 for the lineages passaged in the absence of R and 2 to 22 for those passaged in the presence of R, including in the latter the populations that underwent 30 serial passages in infected cells with R and then five additional passages without R (Fig. 2). The lower average ratios for the R-B series than for the parallel R-A series (Fig. 2B) were confirmed in an independent virus production experiment with the same viral populations. Thus, the results suggest an increase in the capacity to produce progeny in the presence of R for those FMDV populations that had been passaged in the presence of R compared with those passaged in its absence.

**A new mutation in 3D associated with ribavirin resistance.**

To study whether serial passage of FMDV MARLS in the presence of increasing concentrations of R resulted in any alteration of the viral RdRp (3D), RNA from the MARLS-Ap25, MARLS-Ap30, MARLS-Ap35, R-Ap25, R-Ap30, R-Ap35, Ap35, MARLS-Bp25, MARLS-Bp30, MARLS-Bp35 R-Bp25, R-Bp30, R-Bp35, and Bp35 populations (the relationships among these viral populations are depicted in Fig. 1) was subjected to RT-PCR amplification, and the consensus nucleotide sequences for the 3D-coding regions were determined and compared with the sequence of parental MARLS 3D. Several points of heterogeneity (mixtures of two nucleotides at the same genomic position) were observed among the populations analyzed (data not shown), and some of the mutations could contribute to the differences between R-A and R-B populations with regard to the capacity to produce progeny in the presence of R; this possibility could also apply to the differences between Ap35, Bp35, and those populations passaged always in the presence of R. This point was not further investigated (see Discussion). However, the G7497A mutation was the only one found to be established in each of the viral populations subjected to multiple passages in the presence of

R and was absent in each of the populations passaged in the absence of R. The G7497A mutation leads to the amino acid substitution M296I in 3D, suggesting that this replacement was selected in the course of viral replication in the presence of R.

**FMDV 3D with the M296I replacement confers decreased sensitivity to ribavirin.**

The increased capacity of FMDV to produce progeny in the presence of R could be associated with replacement M296I in 3D but also (i) with other genetic modifications of the virus that could interfere with the intracellular activation of R or could decrease the effective concentration of active R derivatives in the replication complex or (ii) with other indirect mechanisms that could compensate for the effect of R. To investigate the possible implication of the 3D substitution M296I in the decreased sensibility to R, plasmids pMT28-3D(M) and pMT28-3D(M-M296I) were constructed and their infectious transcripts were used to transfect BHK-21 cells to rescue FMDV encoding either 3D(M) or 3D(M-M296I) in the same genetic background. The two viruses were compared with regard to progeny production in the absence and presence of R. The results show a modest but significant increase in the progeny production of the virus with 3D(M-M296I) in the presence of R compared with that of the virus encoding 3D(M) in an infection at a low multiplicity of infection (MOI) (Fig. 3A and B). To confirm that pMT28-3D(M-M296I) had a selective replicative advantage over pMT28-3D(M) in the presence of R, the relative fitness of the two viruses was calculated by direct growth competition in BHK-21 cells, in the presence and absence of R. The results (Fig. 4) show a fitness of pMT28-3D(M-M296I) relative to that of pMT28-3D(M) of 3.8 in the presence of 800  $\mu$ M R but of 0.5 in the absence of R. These values indicate a clear replicative advantage of FMDV harboring 3D M296I only in the presence of R, in agreement with the results of progeny production in the presence and absence of R by the two viruses independently (Fig. 2).

Amino acid 232 of 3D is H in FMDV MARLS but Q in FMDV C-S8c1. To investigate whether 3D replacement M296I

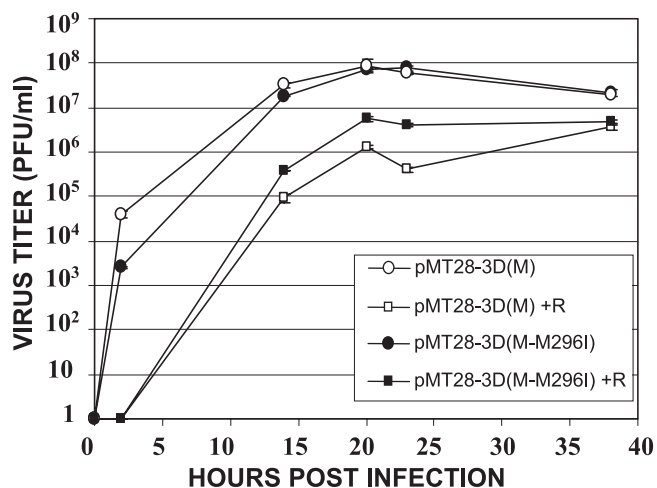


FIG. 3. Infectivity of progeny virus in infections of BHK-21 cells with FMDV encoding either wild-type 3D or 3D with the M296I mutation. Shown are the kinetics of progeny production after infection of BHK-21 cells (MOI of 0.05 PFU/cell) with pMT28-3D(M) or pMT28-3D(M-M296I) in the absence or presence of 800  $\mu$ M R (+R). Procedures are described in Materials and Methods.

conferred a selective advantage in the presence of R and also in the sequence context of C-S8c1 3D (in the absence of 3D replacement Q232H), viruses pMT28 and pMT28-3D(M296I) were rescued from infectious transcripts as described in Materials and Methods. Again, 3D replacement M296I conferred on FMDV C-S8c1 a selective advantage in the presence of R, as evidenced by the results of an infection carried out at a high MOI (2 PFU/cell). The infectious titer produced by the virus rescued from pMT28-3D(M296I) in the presence and absence of R was  $(1.5 \pm 0.4) \times 10^6$  PFU/ml and  $(2.2 \pm 0.4) \times 10^7$  PFU/ml. The corresponding values for virus rescued from pMT28-3D were  $(5.6 \pm 1.1) \times 10^5$  PFU/ml and  $(2.7 \pm 0.4) \times 10^7$  PFU/ml. Thus, the ratio of the level of production of infectious progeny in the presence of R to that in the absence

of R was threefold higher for the virus expressing mutant 3D than for the virus expressing standard 3D.

**Biased mutation types in mutant spectra of ribavirin-treated FMDV.** Previous analyses of clonal populations of FMDV passaged in BHK-21 cells in the absence of mutagens indicated a mutation frequency among components of the mutant spectrum (calculated relative to the consensus sequence of the corresponding populations) of  $0.7 \times 10^{-4}$  up to  $5.9 \times 10^{-4}$  substitutions per nucleotide (1, 57, 68), with a modest dominance of the C→A, C→U, and U→C mutations (Table 1). When persistently infected BHK-21 cells were treated with R, mutation frequencies among components of the mutant spectra in the resident FMDV reached from  $5.7 \times 10^{-4}$  up to  $2.1 \times 10^{-3}$  substitutions per nucleotide (1). The mutation types were highly biased in favor of C→U and G→A (32 out of 40 mutations [1]). To investigate whether a similar mutation type bias was observed in FMDV passaged cytotactically in the presence of R, molecular clones representing the 3D-coding region of the Ap35 and Bp35 populations were sequenced and the mutation types analyzed. The mutation frequency for the two populations was  $1.7 \times 10^{-3}$  substitutions per nucleotide, in agreement with previous determinations from persistent R-treated FMDV infections (1). Again, the results (Table 1) show a dominance of C→U and G→A transitions (96 out of 117 mutations), a statistically significant bias relative to the transitions shown by populations passaged in the absence of R ( $0.005 > P > 0.001$ ;  $\chi^2$  test). The results indicate that the process of the cytotactical replication of FMDV in the presence of R results in the systematic selection of virus harboring the M296I substitution in 3D, accompanied by an increase in mutant spectrum complexity and the dominance of the C→U and G→A transitions.

**Similar mutant spectrum complexities of viruses expressing 3D and 3D(M296I).** To investigate whether the 3D M296I replacement could alter the complexity of the mutant spectrum of the FMDV quasispecies, virus expressing either standard 3D or 3D(M296I) was rescued from infectious transcripts of

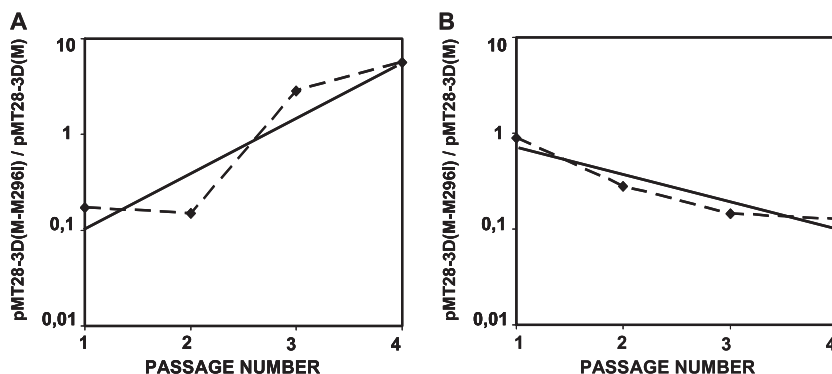


FIG. 4. Relative levels of fitness of FMDVs including either wild-type 3D or 3D(M296I) in the presence or absence of R. (A) BHK-21 cells were infected with a mixture of the clone with wild-type 3D [clone pMT28-3D(M)] and the clone with the M296I mutation in 3D [pMT28-3D(M-M296I)] at a MOI of 0.1 PFU/cell in the presence of 800  $\mu$ M R. The progeny of the first infection was used to infect cells under the same conditions, and the process was repeated a total of four times. (B) Experiments were the same as those whose results are shown in panel A, except that the infections were carried out in the absence of R. The ratio of pMT28-3D(M) to pMT28-3D(M-M296I) was determined for each population by real time RT-PCR using discriminatory primers and control RNAs as detailed in Materials and Methods. Straight lines were fitted to the experimental points; the equations obtained were  $y = 0.0283 \times e^{1.3395x}$  and  $R^2 = 0.8488$  (in the presence of R) and  $y = 1.3305 \times e^{-0.6524x}$  and  $R^2 = 0.8916$  (in the absence of R). The antilogarithm of the vector slope gives the relative levels of fitness of the two competing viruses (49). A second, independent fitness determination gave similar results. Procedures are detailed in Materials and Methods.

TABLE 1. Types of mutations in mutant spectra of FMDV populations passaged in the presence or absence of R

Mutation type	Presence of R					Absence of R				
	Persistent C-S8c1 <sup>a</sup>	Ap35 <sup>b</sup>	Bp35 <sup>c</sup>	pMT28 p5 <sup>d</sup>	pMT28-3D (M296I)p5 <sup>e</sup>	Persistent C-S8c1 <sup>a</sup>	Cytolytic C-S8c1 <sup>f</sup>	Cytolytic C-S8c1 <sup>g</sup>	pMT28 p5 <sup>h</sup>	pMT28-3D (M296I)p5 <sup>i</sup>
A→C	1	0	0	0	0	1	1	0	0	0
A→G	2	1	5	8	0	1	1	0	6	12
A→U	0	1	0	1	1	1	0	0	0	1
C→A	0	1	1	0	0	4	6	0	0	1
C→U	21	20	38	12	4	3	3	3	2	2
G→A	11	10	28	2	6	2	1	0	1	4
G→C	0	1	0	0	0	0	0	0	0	0
G→U	1	0	4	0	0	1	1	0	0	0
U→C	4	3	4	1	3	1	3	0	9	6
U→G	0	0	0	0	0	0	0	0	0	2

<sup>a</sup> Data are from reference 1.

<sup>b</sup> Ap35 is the population described in Results and the legend to Fig. 1. Mutations are based on the analysis of 23 clones (20,010 nucleotides) of genomic residues 7150 to 8020 (3D-coding region).

<sup>c</sup> Bp35 is the population described in Results and the legend to Fig. 1. Mutations are based in the analysis of 47 clones (47,752 nucleotides) of genomic residues 7004 to 8020 (3D-coding region).

<sup>d</sup> Virus expressed from plasmid pMT28 (standard C-S8c1 sequence) passaged five times in BHK-21 cells in the presence of ribavirin (800  $\mu$ M) as described in Materials and Methods. Mutations are based on the sequencing of 32 clones (19,840 nucleotides) of genomic residues 3210 to 3830 (VP1-coding region).

<sup>e</sup> Virus expressed from plasmid pMT28-3D(M296I) (with 3D substitution M296I in the sequence context of C-S8c1) passaged five times in BHK-21 cells in the presence of 800  $\mu$ M R as described in Materials and Methods. Mutations are based on the sequencing of 20 clones (12,200 nucleotides) of genomic residues 3210 to 3830 (VP1-coding region).

<sup>f</sup> Data are from reference 57.

<sup>g</sup> Data are from reference 58.

<sup>h</sup> Virus expressed from plasmid pMT28 (standard C-S8c1 sequence) passaged five times in BHK-21 as described in Materials and Methods. Mutations are based on the sequencing of 29 clones (40,600 nucleotides) of genomic residues 6620 to 8020 (3D-coding region) and 29 clones (17,980 nucleotides) of genomic residues 3210 to 3830 (VP1-coding region).

<sup>i</sup> Virus expressed from plasmid pMT28-3D(M296I) (with 3D substitution M296I in the sequence context of C-S8c1) passaged five times in BHK-21 cells as described in Materials and Methods. Mutations are based on the sequencing of 29 clones (40,600 nucleotides) of genomic residues 6620 to 8020 (3D-coding region) and 29 clones (17,980 nucleotides) of genomic residues 3210 to 3830 (VP1-coding region).

pMT28 or pMT28-3D(M296I), respectively, and passaged five times in BHK-21 cells as described in Materials and Methods. The mutation frequencies of the mutant spectra generated by the viruses expressing the mutant and standard 3Ds were  $4.6 \times 10^{-4}$  and  $3 \times 10^{-4}$  substitutions per nucleotide, respectively. The Shannon entropies of the mutant spectra of the pMT28-3D(M296I) and pMT28 populations were 0.56 and 0.45, respectively. Thus, the results for the complexity of the mutant spectrum do not provide evidence that the M296I replacement enhanced the template copying of FMDV 3D. In parallel passages of the same viruses in the presence of 800  $\mu$ M R, the mutation frequencies in the mutagenized mutant spectra at passage 5 were  $11.5 \times 10^{-4}$  and  $12.1 \times 10^{-4}$  substitutions per nucleotide for the mutant and standard FMDVs, respectively. The Shannon entropies of the mutant spectra generated by the viruses expressing 3D(M296I) and standard 3D in the presence of R were 0.65 and 0.75, respectively. A comparison of mutation frequencies attained in the presence and absence of R indicates that, while the presence of R resulted in a 2.5-fold increase in mutation frequency for the mutant FMDV, the increase for the standard virus was 4-fold. The distribution of mutation types observed (Table 1) does not differ significantly from those recorded for other FMDV populations passaged either in the presence or in the absence of R.

**Mutant polymerase 3D M296I is deficient in the incorporation of ribavirin triphosphate.** The bias toward C→U and G→A (rather than U→C and A→G) transitions in the mutant spectra of FMDV populations passaged in the presence of R suggests a preference for ribavirin monophosphate (RMP) to be incorporated in the place of GMP rather than in the place of AMP during FMDV RNA replication. This preference

could be influenced by the decrease in intracellular GTP levels due to the inhibition of IMP dehydrogenase by RMP (1, 58, 69) or by an intrinsic substrate incorporation bias by the viral polymerase. To test whether 3D(M-M296I) differed from 3D(M) with regard to the capacity to use RTP as a substrate, the two enzymes were expressed in *E. coli*, purified, and tested in several polymerization assays, as detailed in Materials and Methods. The two enzymes were >95% pure as judged by polyacrylamide gel electrophoresis analysis and Coomassie brilliant blue staining and were equally active in our standard poly(rU) synthesis assay (3, 37) [the specific activities for 3D(M) and 3D(M-M296I) were  $172.91 \pm 22.71$  pmol  $\mu$ g<sup>-1</sup> min<sup>-1</sup> and  $177.3 \pm 29.12$  pmol  $\mu$ g<sup>-1</sup> min<sup>-1</sup>, respectively, with an average of 10 determinations for each enzyme]. They were also equally active in the VPg uridylylation assay (35) [ $0.429 \pm 0.082$  pmol  $\mu$ g<sup>-1</sup> min<sup>-1</sup> and  $0.476 \pm 0.104$  pmol  $\mu$ g<sup>-1</sup> min<sup>-1</sup> for 3D(M) and 3D(M-M296I), respectively], and both enzymes bound RNA with the same efficiency as determined by an RNA binding assay (3) [ $33.2 \pm 4.9\%$  and  $32.5 \pm 7.1\%$  of RNA molecules were retarded, respectively, using 1800 nM 3D(M) and 3D(M-M296I)]. We evaluated the relative capacities of 3D(M) and 3D(M-M296I) to incorporate ribavirin in the presence of a low concentration of either GTP or ATP. Using poly(rC)-oligo(dG)<sub>15</sub> as the template-primer and [ $\alpha$ -<sup>32</sup>P]GTP and increasing concentrations of RTP as substrates, 3D(M-M296I) showed a significantly decreased capacity to incorporate RTP in the place of GTP, compared with 3D(M), mainly at a high RTP concentration (Fig. 5A and B). In contrast, in polymerization reactions with poly(rU)-poly(rA)<sub>6</sub> as the template-primer carried out in the presence of Mn<sup>2+</sup>, 3D(M-M296I) showed only a modest decreased capacity to incorpo-

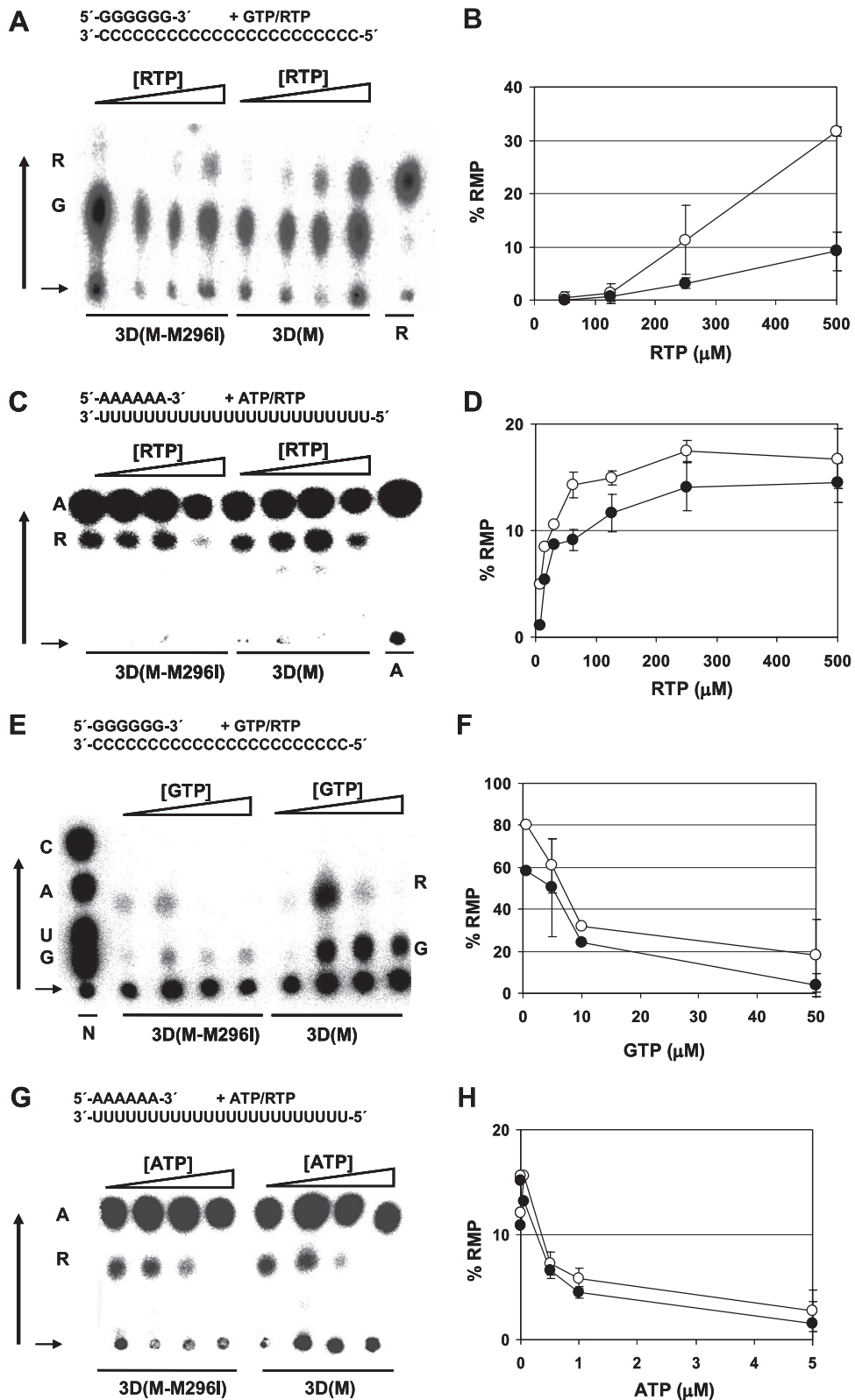


FIG. 5. Incorporation of RMP relative to that of GMP or AMP by purified FMDV 3D(M) or FMDV 3D(M-M296I) using homopolymeric templates-primers. (A) Incorporation of RMP and GMP using poly(rC)-oligo(dG)<sub>15</sub> as the template-primer. The reaction was performed in Mg(CH<sub>3</sub>COO)<sub>2</sub> (15 mM), [α-<sup>32</sup>P]GTP (1 nM), and increasing concentrations of RTP (50, 100, 250, and 500 μM). Results of thin-layer chromatography of RNase-digested products are shown; the black vertical arrow shows the direction of the migration, and the horizontal arrow indicates the sample application point. The positions of ribavirin monophosphate (R) and GMP (G) are indicated. Ribavirin monophosphate control migration is the product of RMP incorporation at position +1 (from the primer 3' end) into sym/sub-RNA 5'-GUACGGGCC-3', with [α-<sup>32</sup>P]UTP incorporated

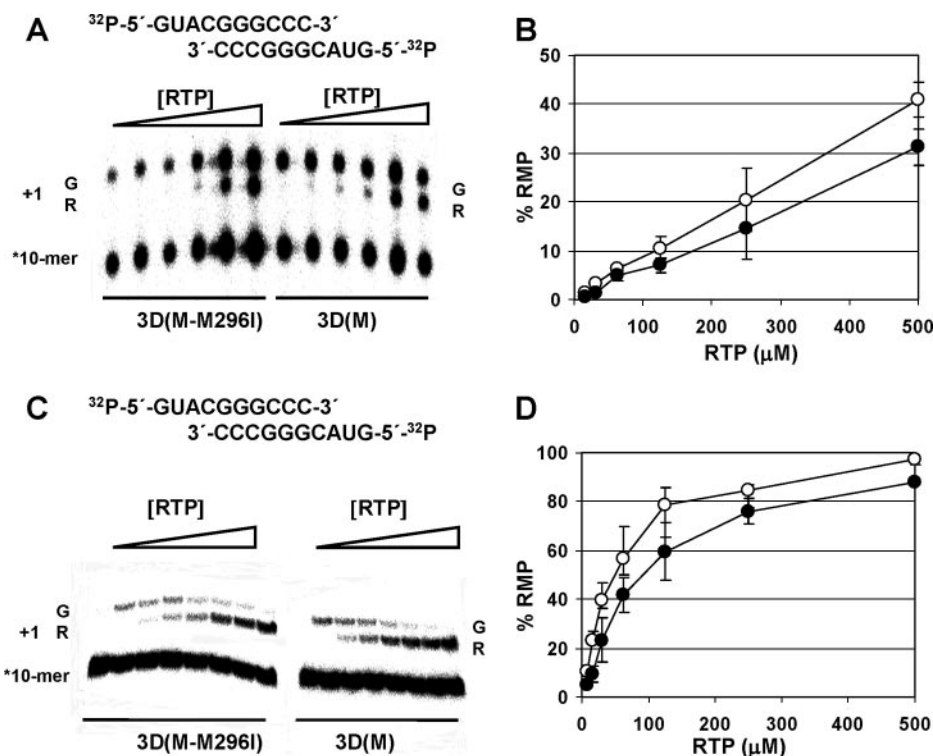


FIG. 6. Relative levels of incorporation of RMP and GMP using a heteropolymeric template-primer. (A) Incorporation of GMP and RMP using the sym/sub-RNA 5'-GUACGGGCC-3' (2 nM),  $\text{Mg}(\text{CH}_3\text{COO})_2$  (15 mM), GTP (10 nM), and RTP (15, 31.25, 62.5, 125, 250, and 500  $\mu\text{M}$ ). Results of denaturing polyacrylamide gel electrophoresis (PAGE) of the  $^{32}\text{P}$ -labeled products from 3D(M) and 3D(M-M296I) polymerase-catalyzed GMP and RMP incorporation are shown. The +1 incorporation position of G and R is indicated. (B) Incorporation of RMP as a function of RTP concentration [ $\circ$ , 3D(M);  $\bullet$ , 3D(M-M296I)]. Averages of results from three experiments performed like that shown in panel A are shown. (C) Incorporation of GMP and RMP using sym/sub-RNA (0.2 nM),  $\text{Mg}(\text{CH}_3\text{COO})_2$  (15 mM), GTP (1 nM), and RTP (7.5, 15, 31.25, 62.5, 125, 250, and 500  $\mu\text{M}$ ). The results of denaturing PAGE of the  $^{32}\text{P}$ -labeled products from 3D(M) and 3D(M-M296I) polymerase-catalyzed GMP and RMP incorporation are shown. (D) Incorporation of RMP as a function of RTP concentration [ $\circ$ , 3D(M);  $\bullet$ , 3D(M-M296I)]. Averages of results of three experiments performed like that shown in panel C (note the different scales in the ordinates between panels B and D) are shown. Standard deviations of densitometry values are given. Procedures are detailed in Materials and Methods.

rate RMP in the place of AMP, compared with 3D(M) (Fig. 5C and D). A similar difference was quantitated in experiments with poly(rC)-oligo(dG)<sub>15</sub> or poly(rU)-poly(rA)<sub>6</sub>, with increasing concentrations of GTP or ATP, respectively, and with a constant concentration of RTP (Fig. 5E to H). In this assay,

under identical Mn ion and template concentrations, RMP is preferentially incorporated in place of GMP (over AMP).

To investigate whether the decreased capacity to incorporate RTP relative to GTP was maintained with a heteropolymeric template, the incorporation of RTP versus GTP was

at position +2. RNase digestion and nucleotide (nearest-neighbor) analysis were performed as detailed in Materials and Methods. (B) Incorporation of RMP as a function of RTP concentration [ $\circ$ , 3D(M);  $\bullet$ , 3D(M-M296I)]. Shown are averages of results from four experiments performed like that whose results are shown in panel A. (C) Incorporation of RMP and AMP using poly(rU)-poly(rA)<sub>6</sub> as the template-primer,  $\text{MnCl}_2$  (10 mM), [ $\alpha$ - $^{32}\text{P}$ ] ATP (1 nM), and increasing concentrations of RTP (62.5, 125, 250, and 500  $\mu\text{M}$ ). The results of thin-layer chromatography of RNase-digested products are shown. The positions of ribavirin monophosphate (R) and AMP (A) are indicated; other symbols are as described for panel A. (D) Incorporation of RMP as a function of RTP concentration [ $\circ$ , 3D(M);  $\bullet$ , 3D(M-M296I)]. Averages of results from three experiments performed like that whose results are shown in panel C (note the different scales in the ordinates between panels B and D). (E) Incorporation of RMP and GMP using poly(rC)-oligo(dG)<sub>15</sub> as the template-primer,  $\text{MnCl}_2$  (10 mM), RTP (400  $\mu\text{M}$ ), and increasing concentrations of [ $\alpha$ - $^{32}\text{P}$ ]GTP (0.5, 5, 10, and 50  $\mu\text{M}$ ). The results of thin-layer chromatography of RNase-digested products are shown. The positions of ribavirin monophosphate (R) and GMP (G) are indicated. The N lane shows the position of nucleoside monophosphates. Other symbols are as described for panel A. (F) Incorporation of RMP as a function of GTP concentration [ $\circ$ , 3D(M);  $\bullet$ , 3D(M-M296I)]. Shown are averages of results of three experiments performed like that whose results are shown in panel E. (G) Incorporation of RMP and AMP using poly(rU)-poly(rA)<sub>6</sub> as the template-primer,  $\text{MnCl}_2$  (10 mM), RTP (400  $\mu\text{M}$ ), and increasing concentrations of [ $\alpha$ - $^{32}\text{P}$ ]ATP (0.05, 0.5, 1, and 5  $\mu\text{M}$ ). Results of thin-layer chromatography of RNase-digested products are shown. The positions of ribavirin monophosphate (R) and AMP (A) are indicated. Other symbols are as described for panel A. (H) Incorporation of RMP as a function of ATP concentration [ $\circ$ , 3D(M);  $\bullet$ , 3D(M-M296I)]. Shown are averages of results from three experiments performed like that whose results are shown in panel G (note the different scales in the ordinates between panels F and H). Standard deviations of densitometry values are given. Procedures are detailed in Materials and Methods.

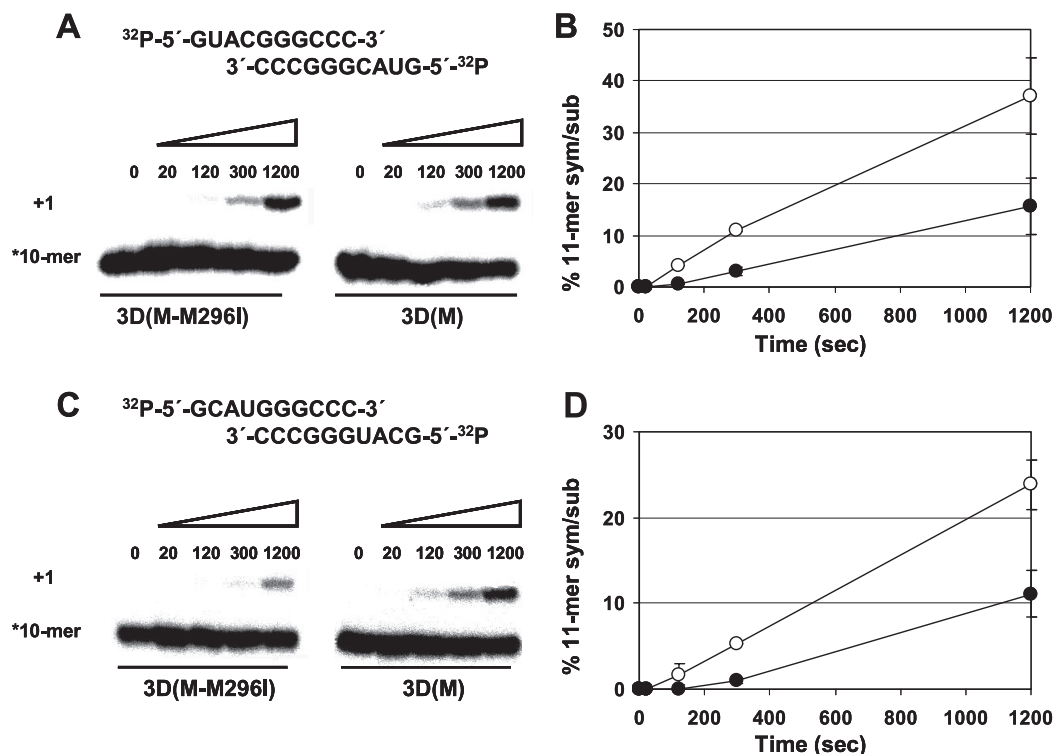


FIG. 7. Incorporation of RMP into sym/sub-C and sym/sub-U by wild-type 3D(M) and mutant 3D(M-M296I). (A) Denaturing PAGE of the  $^{32}\text{P}$ -labeled products of the polymerase-catalyzed RMP incorporation into sym/sub-C. 3D (3  $\mu\text{M}$ ) was mixed with sym/sub-C RNA (0.5  $\mu\text{M}$  duplex) for 10 min for annealing, and then RTP (50  $\mu\text{M}$ ) was added to the reaction mixture. Reactions were stopped at the indicated times by the addition of EDTA. (B) Kinetics (0, 20, 120, 300, and 1,200 s) of RMP incorporation into sym/sub-C by 3D(M) ( $\circ$ ) and 3D(M-M296I) ( $\bullet$ ). Shown are averages of results from three experiments performed like that whose results are shown in panel A. Standard deviations of densitometry values are given. (C and D) Experiments were performed and symbols are the same as those described for panels A and B, respectively, except that sym/sub-U was used as the template-primer. Procedures are detailed in Materials and Methods.

tested with a sym/sub-RNA template-primer at a defined (+1) template position (Fig. 6A to D). Under two different reaction conditions, 3D(M-M296I) showed a significantly lower capacity than wild-type 3D(M) to incorporate RMP in the place of GMP, in agreement with results using homopolymeric templates-primers. To examine how efficiently FMDV polymerase incorporates RMP when mimicking GTP or ATP, we measured the incorporation of RMP into sym/sub-C and sym/sub-U in the absence of standard nucleotides. The results (Fig. 7) show again that RMP was more efficiently incorporated with C as a template than with U. With the two templates, mutant 3D(M-M296I) incorporated RMP less efficiently than wild-type 3D(M), in agreement with the results of a competitive incorporation of RMP relative to GMP and AMP. Thus, the enzymological measurements agree with the virological studies and support the conclusion that FMDV polymerase with decreased sensitivity to R was selected upon passage of the virus in the presence of R.

## DISCUSSION

**New picornaviral RdRp with decreased sensitivity to ribavirin.** Previous results indicated that R is mutagenic for FMDV (1). Here we have reported that serial infections in the presence of increasing concentrations of R resulted in the selection of FMDV with a decreased sensitivity to R. The mutant spec-

tra of FMDV populations passaged in the presence of R showed elevated mutation frequencies, which reflected a continued mutagenic action of R, with a highly significant increase in the proportion of the transitions C $\rightarrow$ U and G $\rightarrow$ A relative to other mutation types (Table 1). This suggests a preference for RTP to be incorporated in place of GTP rather than in place of ATP by FMDV 3D or that UTP is incorporated more frequently than CTP when R is present in template RNA (1). Since R treatment of BHK-21 cells results in sustained intracellular levels of about 5 fmol/cell, while GTP levels are decreased to about 1 fmol/cell (1), an environmental pressure to misincorporate RTP instead of GTP is likely to be a selective force acting on FMDV while it replicates in the presence of R. This selective force may have contributed to the establishment of FMDV with substitution M296I in 3D. That this replacement was the result of selection by the presence of R is indicated by its dominance only in the FMDV MARLS quasispecies that replicated in the presence of R and not in the two MARLS quasispecies passaged in parallel in the absence of R (Fig. 1). M296I was not found in several mutant spectra of other FMDV lineages (large population passages or plaque-to-plaque transfers) in which replication occurred either in the absence of mutagens or in the presence of 5-fluorouracil or 5-azacytidine (31, 32, 55, 57, 68). Furthermore, substitution M296I in 3D conferred a selective advantage on FMDV—in the sequence context of either C-S8c1 or MARLS—in the

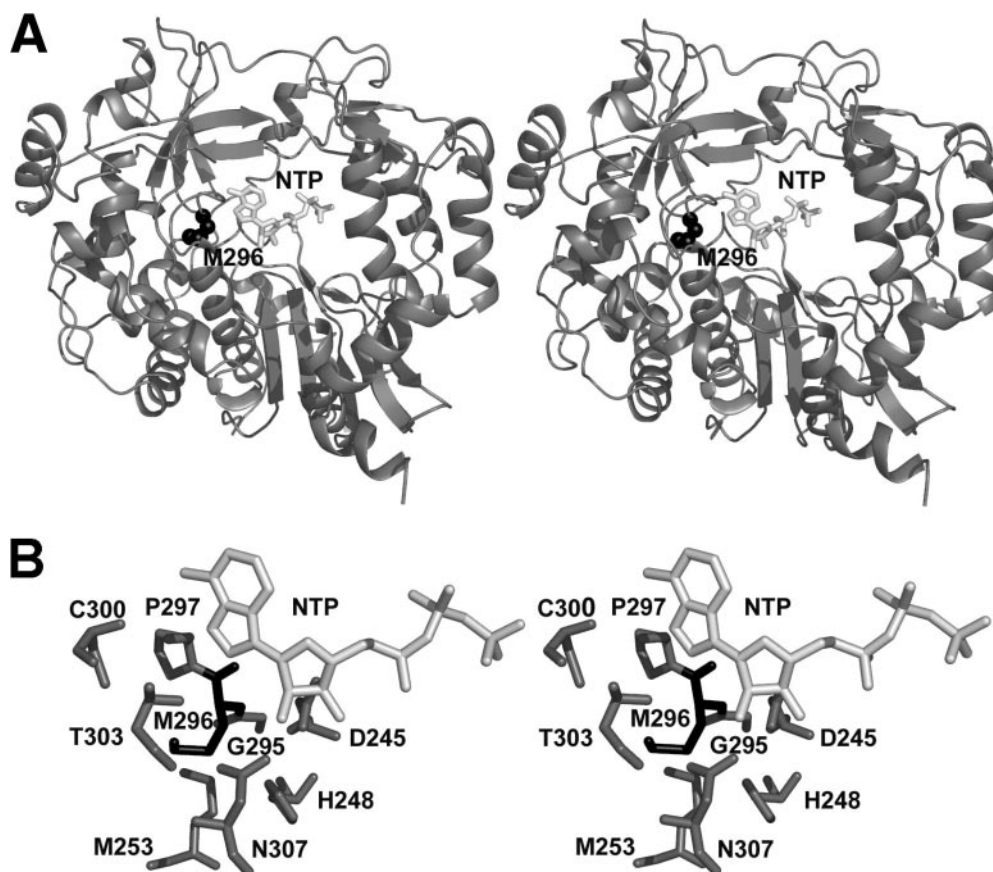


FIG. 8. Stereoviews of the location of M296 in the polymerase (3D) of FMDV. (A) Ribbon diagram of the structure of FMDV 3D that shows the location of M296 (the representation of CPK is in black) and an incoming nucleoside triphosphate (NTP) (white sticks). The structure corresponds to a complex with a template-primer; the incoming nucleotide is modeled as previously reported (35, 37). M296 is located in a loop connecting strand  $\beta$ 9 and the  $\alpha$ 11 helix (37). The sequence of this loop is highly conserved in picornaviral polymerases. (B) Diagram showing the amino acids that are in direct contact with M296. The modeled NTP is also shown as a reference. M296 does not have direct interactions with the template-primer RNA or with the incoming NTP. However, this residue is in close contact (distance, lower than 3.5 Å) with amino acids D245 and N307, both of which play an important role in the positioning of the incoming nucleotide substrate by direct hydrogen bonding of their side chains to the ribose 2' hydroxyl group (35, 37). M296 is also close to residues S298, C300, and T303, which might contact the NTP base (37). Diagrams are courtesy of N. Verdaguier (IBM-CSIC, Barcelona, Spain).

presence of R but not in its absence (Fig. 3). The differences in levels of sensitivity to R observed for the viral populations Ap35 and Bp35 (Fig. 1) despite similar high mutation frequencies could be due to differences in the mutant spectrum compositions of the two populations or to mutation frequencies approaching a plateau level compatible with continuing viral replication.

The fitness value of FMDV expressing 3D(M-M296I) relative to FMDV expressing 3D(M) was increased 7.6-fold in the presence of R, with respect to the value in the absence of R. The fitness cost of 3D replacement M296I was moderated (about twofold) (Fig. 4) and permitted the dominance of FMDV with 3D replacement M296I after five passages in the absence of R (populations Ap35 and Bp35 in Fig. 1).

The evolutionary behavior of FMDV in response to R is in agreement with biochemical data. Polymerization assays with 3D(M) and 3D(M-M296I) using homopolymeric and heteropolymeric templates-primers in the presence of  $Mg^{2+}$  or  $Mn^{2+}$  (3, 5, 37) suggest that at least part of the phenotypic behavior of FMDV associated with 3D substitution M296I is due to a

decreased capacity to incorporate RTP during RNA synthesis (Fig. 5 and 6). In polymerization assays with poly(rC)-poly(dG)<sub>15</sub> in the presence of  $Mn^{2+}$ , we observed the maximum capacity to incorporate RMP, in agreement with previously documented decreases in the copying fidelity of RdRps in the presence of  $Mn^{2+}$  (6, 7, 12). In the presence of  $Mg^{2+}$ , there was no polymerization activity with poly(rU)-poly(rA)<sub>6</sub>, and therefore we have not been able to compare the effects of a divalent ion in this system. In the incorporation assays used, either with RTP in competition with GTP or ATP, which resembles the physiological situation (Fig. 5 and 6), or with RTP alone (Fig. 7), RMP was incorporated in the place of GMP more preferentially than in the place of AMP. The maximum difference between 3D(M) and 3D(M-M296I) was seen in their relative capacities to use RTP instead of GTP as a substrate with homopolymeric templates (Fig. 5); technical problems impeded measurements of incorporation of RMP in the place of AMP using a heteropolymeric template. However, a difference between the two enzymes was also seen in the kinetics of incorporation of RMP with sym/sub-C and sym/

sub-U as templates-primers (Fig. 7). Additional studies are necessary to investigate the behavior of FMDV 3D when R is present in template RNA. Determinations of kinetic parameters are required to try to define the step in nucleotide incorporation affected by replacement M296I and to further evaluate whether the decreased incorporation of RMP by 3D(M-M296I) reflects a general alteration in the copying fidelity (decreased misincorporation of a standard nucleotide) by this enzyme. Also, phenotypic assays are in progress to evaluate whether 3D replacement M296I alters the adaptability of FMDV quasispecies in the face of other selective constraints.

An effect of M296I in nucleotide incorporation is not surprising in view of the location of M296I within an amino acid stretch (3D residues 295 to 299) which is highly conserved among picornaviral 3Ds and other RdRps (37). This conserved stretch includes S298, which interacts with template-primer RNA and is predicted to interact with the incoming nucleotide (37). Moreover, 3D residues 300 to 307 (which are part of helix  $\alpha$ 11) include amino acids which either establish contacts with RNA or, again, are predicted to interact with the incoming nucleotide substrate (37) (Fig. 8). Therefore, M296I may exert some influence on the discrimination of standard nucleotides or nucleotide analogues, and structural and enzymological studies to explore this possibility are in progress.

**At least two domains of picornavirus 3D can affect RMP incorporation, with implications for error catastrophe as an antiviral strategy.** Viral extinction through error catastrophe or lethal mutagenesis has been supported by many experimental results and by theoretical studies when the latter are based on realistic assumptions such as the coexistence of genomes with different fitness levels in the mutant spectrum (10, 11, 17, 18, 28, 29, 43, 54, 71; see reviews in references 2 and 27). The transition toward viral extinction occurs with a decrease of specific infectivity, an increase in the complexity of the mutant spectrum, and an invariant consensus sequence of the viral genome (18, 19, 42, 46, 55, 56, 68), a set of properties that distinguish extinction associated with error catastrophe from extinction due solely to the inhibition of viral replication. Furthermore, direct experimental evidence indicates that mutagenesis is required to produce viral extinction (55, 57). Recent developments include evidence of the mutagenic activity of ribavirin in the course of a successful treatment of patients chronically infected with hepatitis C virus (9, 78) and the initiation of a clinical trial with AIDS patients involving the administration of a nucleoside analogue (48).

A poliovirus mutant with replacement G64S in 3D showing decreased sensitivity to R was isolated, and its RdRp has been characterized (8, 62). The mutant enzyme showed an increased template-copying fidelity, produced poliovirus populations with a less complex mutant spectrum than the wild-type enzyme, and rendered the viral quasispecies less adaptable to a complex environment (61, 76). Enzyme catalysis studies suggest that replacement G64S may induce a conformational change in 3D that precedes the phosphoryl transfer during nucleotide incorporation (8). Unlike replacement M296I in FMDV 3D, replacement G64S in poliovirus 3D lies far from residues involved directly in template recognition and nucleotide binding (8, 36, 37, 74). It has been suggested that G64, located in the finger domain of poliovirus 3D, is hydrogen bonded to residues which in turn are hydrogen bonded to 3D

motif A, which includes residues that bind metal ions or interact with the ribose moiety of the incoming nucleotide. The perturbation of motif A as a result of G64S may alter the equilibrium position of the triphosphate and the fidelity properties of the enzyme (8).

Two groups independently isolated the same G64S 3D poliovirus mutation, affecting a residue that does not interact directly with the incoming nucleotide (62, 75). The isolation of the M296I mutation in FMDV 3D, however, suggests that the occurrence of picornavirus mutants with a decreased capacity to incorporate RTP (and perhaps other nucleotide analogues) may not be as restricted as suggested by the results with poliovirus. Substitutions at different enzyme domains may lead to related mutagen-resistant phenotypes, which could contribute to failures in the event of an application of lethal mutagenesis as an antiviral strategy. RdRp mutations that confer a decreased sensitivity of hepatitis C virus to R *in vivo* have been reported (78). One possibility is that, when the intensity of the mutagenic activity is sufficient, no extinction escape mutants will be selected (55, 57, 72). Noticeably, the isolation of FMDV with decreased sensitivity to R was achieved by passaging the virus in the presence of increasing concentrations of R (Fig. 1). Genomes encoding 3D replacement M296I were not detected in the mutant spectra of FMDV treated directly with high R concentrations on the way to extinction (1). In this view, the situation would have a parallel in the isolation of inhibitor escape viral variants, which is favored by suboptimal inhibitory concentrations (52). Weighing against selection of extinction escape mutants in lethal mutagenesis is the interfering effect of mutagenized mutant spectra (20, 41, 47). More work is needed to clarify the tolerance of viral polymerases to accept replacements that enhance viral resistance to mutagenic agents and to evaluate to what extent such replacements can affect the efficacy of lethal mutagenesis. Interestingly, mutagen-resistant polymerase mutants may offer a tool for understanding the molecular basis of template-copying fidelity and to design new fidelity-lowering drugs to become components of formulations for lethal mutagenesis (2, 27, 48, 51).

#### ACKNOWLEDGMENTS

We are indebted to C. Escarmís for the supply of infectious FMDV clones and valuable advice, to N. Verdaguier for information on the structures of 3D and 3D complexes and for the preparation of Fig. 8, to M. Dávila for expert technical assistance, and to J. C. de la Torre for supplying ribavirin.

This work was supported by grant BFU-2005-00863 from MCyT, by grant 08.2/0015/2001 from CAM, and by the Fundación R. Arecas. M.S. was supported by a predoctoral fellowship from the Ministerio de Educación y Ciencia, A. Airaksinen by a Marie Curie Fellowship of the European Community program Quality of Life and Management of Living Resources under contract QLK2-CT-1999-51462, C.G.-L. by a postdoctoral fellowship from CAM, R.A. by a predoctoral fellowship from CAM, and A. Arias by a postdoctoral contract under Proyecto Intramural de Frontera (CSIC, 2005).

#### REFERENCES

1. Airaksinen, A., N. Pariente, L. Menendez-Arias, and E. Domingo. 2003. Curing of foot-and-mouth disease virus from persistently infected cells by ribavirin involves enhanced mutagenesis. *Virology* **311**:339–349.
2. Anderson, J. P., R. Daifuku, and L. A. Loeb. 2004. Viral error catastrophe by mutagenic nucleosides. *Annu. Rev. Microbiol.* **58**:183–205.
3. Arias, A., R. Agudo, C. Ferrer-Orta, R. Perez-Luque, A. Airaksinen, E. Brocchi, E. Domingo, N. Verdaguier, and C. Escarmís. 2005. Mutant viral polymerase in the transition of virus to error catastrophe identifies a critical site for RNA binding. *J. Mol. Biol.* **353**:1021–1032.

4. Arias, A., C. M. Ruiz-Jarabo, C. Escarmis, and E. Domingo. 2004. Fitness increase of memory genomes in a viral quasispecies. *J. Mol. Biol.* **339**:405–412.
5. Arnold, J. J., and C. E. Cameron. 2000. Poliovirus RNA-dependent RNA polymerase (3D<sup>pol</sup>). Assembly of stable, elongation-competent complexes by using a symmetrical primer-template substrate (sym/sub). *J. Biol. Chem.* **275**:5329–5336.
6. Arnold, J. J., S. K. Ghosh, and C. E. Cameron. 1999. Poliovirus RNA-dependent RNA polymerase (3D<sup>pol</sup>). Divalent cation modulation of primer, template, and nucleotide selection. *J. Biol. Chem.* **274**:37060–37069.
7. Arnold, J. J., D. W. Gohara, and C. E. Cameron. 2004. Poliovirus RNA-dependent RNA polymerase (3D<sup>pol</sup>): pre-steady-state kinetic analysis of ribonucleotide incorporation in the presence of Mn<sup>2+</sup>. *Biochemistry* **43**: 5138–5148.
8. Arnold, J. J., M. Vignuzzi, J. K. Stone, R. Andino, and C. E. Cameron. 2005. Remote site control of an active site fidelity checkpoint in a viral RNA-dependent RNA polymerase. *J. Biol. Chem.* **280**:25706–25716.
9. Asahina, Y., N. Izumi, N. Enomoto, M. Uchihara, M. Kurosaki, Y. Onuki, Y. Nishimura, K. Ueda, K. Tsuchiya, H. Nakanishi, T. Kitamura, and S. Miyake. 2005. Mutagenic effects of ribavirin and response to interferon/ribavirin combination therapy in chronic hepatitis C. *J. Hepatol.* **43**:623–629.
10. Biebricher, C. K., and M. Eigen. 2005. The error threshold. *Virus Res.* **107**:117–127.
11. Biebricher, C. K., and M. Eigen. 2006. What is a quasispecies? *Curr. Top. Microbiol. Immunol.* **299**:1–31.
12. Castro, C., J. J. Arnold, and C. E. Cameron. 2005. Incorporation fidelity of the viral RNA-dependent RNA polymerase: a kinetic, thermodynamic and structural perspective. *Virus Res.* **107**:141–149.
13. Charpentier, N., M. Dávila, E. Domingo, and C. Escarmis. 1996. Long-term, large-population passage of aphthovirus can generate and amplify defective noninterfering particles deleted in the leader protease gene. *Virology* **223**: 10–18.
14. Chumakov, K. M., L. B. Powers, K. E. Noonan, I. B. Roninson, and I. S. Levenbook. 1991. Correlation between amount of virus with altered nucleotide sequence and the monkey test for acceptability of oral poliovirus vaccine. *Proc. Natl. Acad. Sci. USA* **88**:199–203.
15. Cline, J., J. C. Braman, and H. H. Hogrefe. 1996. PCR fidelity of pfu DNA polymerase and other thermostable DNA polymerases. *Nucleic Acids Res.* **24**:3546–3551.
16. Contreras, A. M., Y. Hiasa, W. He, A. Terella, E. V. Schmidt, and R. T. Chung. 2002. Viral RNA mutations are region specific and increased by ribavirin in a full-length hepatitis C virus replication system. *J. Virol.* **76**: 8505–8517.
17. Crotty, S., C. Cameron, and R. Andino. 2002. Ribavirin's antiviral mechanism of action: lethal mutagenesis? *J. Mol. Med.* **80**:86–95.
18. Crotty, S., C. E. Cameron, and R. Andino. 2001. RNA virus error catastrophe: direct molecular test by using ribavirin. *Proc. Natl. Acad. Sci. USA* **98**:6895–6900.
19. Crotty, S., D. Maag, J. J. Arnold, W. Zhong, J. Y. N. Lau, Z. Hong, R. Andino, and C. E. Cameron. 2000. The broad-spectrum antiviral ribonucleotide, ribavirin, is an RNA virus mutagen. *Nat. Med.* **6**:1375–1379.
20. Crowder, S., and K. Kirkegaard. 2005. Trans-dominant inhibition of RNA viral replication can slow growth of drug-resistant viruses. *Nat. Genet.* **37**: 701–709.
21. Day, C. W., D. F. Smee, J. G. Julander, V. F. Yamshchikov, R. W. Sidwell, and J. D. Morrey. 2005. Error-prone replication of West Nile virus caused by ribavirin. *Antivir. Res.* **67**:38–45.
22. de la Torre, J. C., B. Alarcón, E. Martínez-Salas, L. Carrasco, and E. Domingo. 1987. Ribavirin cures cells of a persistent infection with foot-and-mouth disease virus in vitro. *J. Virol.* **61**:233–235.
23. de la Torre, J. C., and J. J. Holland. 1990. RNA virus quasispecies populations can suppress vastly superior mutant progeny. *J. Virol.* **64**:6278–6281.
24. Domingo, E. (ed.). 2006. Current topics in microbiology and immunology, vol. 299. Quasispecies: concepts and implications for virology. Springer-Verlag, Berlin, Germany.
25. Domingo, E., C. Biebricher, M. Eigen, and J. J. Holland. 2001. Quasispecies and RNA virus evolution: principles and consequences. Landes Bioscience, Austin, TX.
26. Domingo, E., M. Dávila, and J. Ortín. 1980. Nucleotide sequence heterogeneity of the RNA from a natural population of foot-and-mouth-disease virus. *Gene* **11**:333–346.
27. Domingo, E. (ed.). 2005. Virus entry into error catastrophe as a new antiviral strategy. *Virus Res.* **107**:115–228.
28. Eigen, M. 2002. Error catastrophe and antiviral strategy. *Proc. Natl. Acad. Sci. USA* **99**:13374–13376.
29. Eigen, M., and C. K. Biebricher. 1988. Sequence space and quasispecies distribution, p. 211–245. *In* E. Domingo, P. Ahlquist, and J. J. Holland (ed.), RNA genetics, vol. 3. CRC Press, Boca Raton, FL.
30. Eigen, M., and P. Schuster. 1979. The hypercycle. A principle of natural self-organization. Springer, Berlin, Germany.
31. Escarmis, C., M. Dávila, N. Charpentier, A. Bracho, A. Moya, and E. Domingo. 1996. Genetic lesions associated with Muller's ratchet in an RNA virus. *J. Mol. Biol.* **264**:255–267.
32. Escarmis, C., G. Gómez-Mariano, M. Dávila, E. Lázaro, and E. Domingo. 2002. Resistance to extinction of low fitness virus subjected to plaque-to-plaque transfers: diversification by mutation clustering. *J. Mol. Biol.* **315**: 647–661.
33. Farci, P., A. Shimoda, A. Coiana, G. Diaz, G. Peddis, J. C. Melpolder, A. Strazzer, D. Y. Chien, S. J. Munoz, A. Balestrieri, R. H. Purcell, and H. J. Alter. 2000. The outcome of acute hepatitis C predicted by the evolution of the viral quasispecies. *Science* **288**:339–344.
34. Farci, P., R. Strazzer, H. J. Alter, S. Farci, D. Degioannis, A. Coiana, G. Peddis, F. Usai, G. Serra, L. Chessa, G. Diaz, A. Balestrieri, and R. H. Purcell. 2002. Early changes in hepatitis C viral quasispecies during interferon therapy predict the therapeutic outcome. *Proc. Natl. Acad. Sci. USA* **99**:3081–3086.
35. Ferrer-Orta, C., A. Arias, R. Agudo, R. Perez-Luque, C. Escarmis, E. Domingo, and N. Verdaguier. 2006. The structure of a protein primer-polymerase complex in the initiation of genome replication. *EMBO J.* **25**:880–888.
36. Ferrer-Orta, C., A. Arias, C. Escarmis, and N. Verdaguier. 2006. A comparison of viral RNA-dependent RNA polymerases. *Curr. Opin. Struct. Biol.* **16**:27–34.
37. Ferrer-Orta, C., A. Arias, R. Perez-Luque, C. Escarmis, E. Domingo, and N. Verdaguier. 2004. Structure of foot-and-mouth disease virus RNA-dependent RNA polymerase and its complex with a template-primer RNA. *J. Biol. Chem.* **279**:47212–47221.
38. Figlerowicz, M., M. Alejska, A. Kurzynska-Kokorniak, and M. Figlerowicz. 2003. Genetic variability: the key problem in the prevention and therapy of RNA-based virus infections. *Med. Res. Rev.* **23**:488–518.
39. García-Arriaza, J., E. Domingo, and C. Escarmis. 2005. A segmented form of foot-and-mouth disease virus interferes with standard virus: a link between interference and competitive fitness. *Virology* **335**:155–164.
40. García-Arriaza, J., S. C. Manrubia, M. Toja, E. Domingo, and C. Escarmis. 2004. Evolutionary transition toward defective RNAs that are infectious by complementation. *J. Virol.* **78**:11678–11685.
41. González-López, C., A. Arias, N. Pariente, G. Gómez-Mariano, and E. Domingo. 2004. Preextinction viral RNA can interfere with infectivity. *J. Virol.* **78**:3319–3324.
42. González-López, C., G. Gómez-Mariano, C. Escarmis, and E. Domingo. 2005. Invariant aphthovirus consensus nucleotide sequence in the transition to error catastrophe. *Infect. Genet. Evol.* **5**:366–374.
43. Graci, J. D., and C. E. Cameron. 2004. Challenges for the development of ribonucleoside analogues as inducers of error catastrophe. *Antivir. Chem. Chemother.* **15**:1–13.
44. Graci, J. D., and C. E. Cameron. 2006. Mechanisms of action of ribavirin against distinct viruses. *Rev. Med. Virol.* **16**:37–48.
45. Graci, J. D., and C. E. Cameron. 2002. Quasispecies, error catastrophe, and the antiviral activity of ribavirin. *Virology* **298**:175–180.
46. Grande-Pérez, A., G. Gómez-Mariano, P. R. Lowenstein, and E. Domingo. 2005. Mutagenesis-induced, large fitness variations with an invariant arenavirus consensus genomic nucleotide sequence. *J. Virol.* **79**:10451–10459.
47. Grande-Pérez, A., E. Lázaro, P. Lowenstein, E. Domingo, and S. C. Manrubia. 2005. Suppression of viral infectivity through lethal defection. *Proc. Natl. Acad. Sci. USA* **102**:4448–4452.
48. Harris, K. S., W. Brabant, S. Styrchak, A. Gall, and R. Daifuku. 2005. KP-1212/1461, a nucleoside designed for the treatment of HIV by viral mutagenesis. *Antivir. Res.* **67**:1–9.
49. Holland, J. J., J. C. de la Torre, D. K. Clarke, and E. Duarte. 1991. Quantitation of relative fitness and great adaptability of clonal populations of RNA viruses. *J. Virol.* **65**:2960–2967.
50. Lanford, R. E., D. Chavez, B. Guerra, J. Y. Lau, Z. Hong, K. M. Brasky, and B. Beames. 2001. Ribavirin induces error-prone replication of GB virus B in primary tamarin hepatocytes. *J. Virol.* **75**:8074–8081.
51. Loeb, L. A., J. M. Essigmann, F. Kazazi, J. Zhang, K. D. Rose, and J. I. Mullins. 1999. Lethal mutagenesis of HIV with mutagenic nucleoside analogs. *Proc. Natl. Acad. Sci. USA* **96**:1492–1497.
52. Menéndez-Arias, L. 2002. Targeting HIV: antiretroviral therapy and development of drug resistance. *Trends Pharmacol. Sci.* **23**:381–388.
53. Moreno, I. M., J. M. Malpica, E. Rodríguez-Cerezo, and F. García-Arenal. 1997. A mutation in tomato aspermy cucumovirus that abolishes cell-to-cell movement is maintained to high levels in the viral RNA population by complementation. *J. Virol.* **71**:9157–9162.
54. Nowak, M., and P. Schuster. 1989. Error thresholds of replication in finite population mutation frequencies and the onset of Muller's ratchet. *J. Theor. Biol.* **137**:375–395.
55. Pariente, N., A. Airaksinen, and E. Domingo. 2003. Mutagenesis versus inhibition in the efficiency of extinction of foot-and-mouth disease virus. *J. Virol.* **77**:7131–7138.
56. Pariente, N., S. Sierra, and A. Airaksinen. 2005. Action of mutagenic agents and antiviral inhibitors on foot-and-mouth disease virus. *Virus Res.* **107**:183–193.
57. Pariente, N., S. Sierra, P. R. Lowenstein, and E. Domingo. 2001. Efficient

- virus extinction by combinations of a mutagen and antiviral inhibitors. *J. Virol.* **75**:9723–9730.
58. **Parker, W. B.** 2005. Metabolism and antiviral activity of ribavirin. *Virus Res.* **107**:165–171.
  59. **Pawlotsky, J. M.** 2006. Hepatitis C virus population dynamics during infection. *Curr. Top. Microbiol. Immunol.* **299**:261–284.
  60. **Pawlotsky, J. M.** 2000. Hepatitis C virus resistance to antiviral therapy. *Hepatology* **32**:889–896.
  61. **Pfeiffer, J. K., and K. Kirkegaard.** 2005. Increased fidelity reduces poliovirus fitness under selective pressure in mice. *PLoS Pathog.* **1**:102–110.
  62. **Pfeiffer, J. K., and K. Kirkegaard.** 2003. A single mutation in poliovirus RNA-dependent RNA polymerase confers resistance to mutagenic nucleotide analogs via increased fidelity. *Proc. Natl. Acad. Sci. USA* **100**:7289–7294.
  63. **Quer, J., J. I. Esteban, J. Cos, S. Sauleda, L. Ocana, M. Martell, T. Otero, M. Cubero, E. Palou, P. Murillo, R. Esteban, and J. Guardia.** 2005. Effect of bottlenecks on evolution of the nonstructural protein 3 gene of hepatitis C virus during sexually transmitted acute resolving infection. *J. Virol.* **79**:15131–15141.
  64. **Rowe, C. L., S. C. Baker, M. J. Nathan, and J. O. Fleming.** 1997. Evolution of mouse hepatitis virus: detection and characterization of spike deletion variants during persistent infection. *J. Virol.* **71**:2959–2969.
  65. **Ruiz-Jarabo, C. M., C. Ly, E. Domingo, and J. C. de la Torre.** 2003. Lethal mutagenesis of the prototypic arenavirus lymphocytic choriomeningitis virus (LCMV). *Virology* **308**:37–47.
  66. **Sambrook, J., and D. W. Russell.** 2001. *Molecular cloning: a laboratory manual*, 3rd ed. Cold Spring Harbor Laboratory Press, Cold Spring Harbor, NY.
  67. **Severson, W. E., C. S. Schmaljohn, A. Javadian, and C. B. Jonsson.** 2003. Ribavirin causes error catastrophe during Hantaan virus replication. *J. Virol.* **77**:481–488.
  68. **Sierra, S., M. Dávila, P. R. Lowenstein, and E. Domingo.** 2000. Response of foot-and-mouth disease virus to increased mutagenesis. Influence of viral load and fitness in loss of infectivity. *J. Virol.* **74**:8316–8323.
  69. **Snell, N. J.** 2001. Ribavirin—current status of a broad spectrum antiviral agent. *Expert Opin. Pharmacother.* **2**:1317–1324.
  70. **Sobrinho, F., M. Dávila, J. Ortín, and E. Domingo.** 1983. Multiple genetic variants arise in the course of replication of foot-and-mouth disease virus in cell culture. *Virology* **128**:310–318.
  71. **Swetina, J., and P. Schuster.** 1982. Self-replication with errors. A model for polynucleotide replication. *Biophys. Chem.* **16**:329–345.
  72. **Tapia, N., G. Fernandez, M. Parera, G. Gomez-Mariano, B. Clotet, M. Quinones-Mateu, E. Domingo, and M. A. Martínez.** 2005. Combination of a mutagenic agent with a reverse transcriptase inhibitor results in systematic inhibition of HIV-1 infection. *Virology* **338**:1–8.
  73. **Teng, M. N., M. B. Oldstone, and J. C. de la Torre.** 1996. Suppression of lymphocytic choriomeningitis virus-induced growth hormone deficiency syndrome by disease-negative virus variants. *Virology* **223**:113–119.
  74. **Thompson, A. A., and O. B. Peersen.** 2004. Structural basis for proteolysis-dependent activation of the poliovirus RNA-dependent RNA polymerase. *EMBO J.* **23**:3462–3471.
  75. **Vignuzzi, M., J. K. Stone, and R. Andino.** 2005. Ribavirin and lethal mutagenesis of poliovirus: molecular mechanisms, resistance and biological implications. *Virus Res.* **107**:173–181.
  76. **Vignuzzi, M., J. K. Stone, J. J. Arnold, C. E. Cameron, and R. Andino.** 2006. Quasispecies diversity determines pathogenesis through cooperative interactions in a viral population. *Nature* **439**:344–348.
  77. **Volckaert, G., and W. Fiers.** 1977. Micro thin-layer techniques for rapid sequence analysis of 32P-labeled RNA: double digestion and pancreatic ribonuclease analyses. *Anal. Biochem.* **83**:228–239.
  78. **Young, K. C., K. L. Lindsay, K. J. Lee, W. C. Liu, J. W. He, S. L. Milstein, and M. M. Lai.** 2003. Identification of a ribavirin-resistant NS5B mutation of hepatitis C virus during ribavirin monotherapy. *Hepatology* **38**:869–878.